

**UNCLASSIFIED**

**AD 407 784**

**DEFENSE DOCUMENTATION CENTER**

**FOR**

**SCIENTIFIC AND TECHNICAL INFORMATION**

**CAMERON STATION, ALEXANDRIA, VIRGINIA**



**UNCLASSIFIED**

NOTICE: When government or other drawings, specifications or other data are used for any purpose other than in connection with a definitely related government procurement operation, the U. S. Government thereby incurs no responsibility, nor any obligation whatsoever; and the fact that the Government may have formulated, furnished, or in any way supplied the said drawings, specifications, or other data is not to be regarded by implication or otherwise as in any manner licensing the holder or any other person or corporation, or conveying any rights or permission to manufacture, use or sell any patented invention that may in any way be related thereto.

63-4-2

DI-82-0242

CATALOGED BY DDC

AS AD NO. 407784

# BOEING SCIENTIFIC RESEARCH LABORATORIES

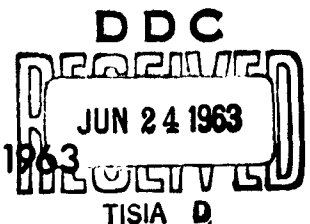
On the Optimum Transversal Contour  
of a Body at Hypersonic Speeds

407784

Angelo Miele

Gary R. Saaris

March 1963



**D1-82-0242**

**BOEING SCIENTIFIC RESEARCH LABORATORIES  
FLIGHT SCIENCES LABORATORY TECHNICAL REPORT NO. 73**

**ON THE OPTIMUM TRANSVERSAL CONTOUR  
OF A BODY AT HYPERSONIC SPEEDS**

**ANGELO MIELE AND GARY R. SAARIS**

**MARCH 1963**

TABLE OF CONTENTS

## Summary

1. Introduction
2. Determination of the drag
3. Formulation of the problem
  - 3.1. Necessary conditions
  - 3.2. Symmetry and multiplicity properties
4. Multiple and symmetric solutions
  - 4.1. Bodies of class I
  - 4.2. Bodies of class II
  - 4.3. Bodies of class III
  - 4.4. Discussion of the results
5. General solutions

## References

ON THE OPTIMUM TRANSVERSAL CONTOUR  
OF A BODY AT HYPERSONIC SPEEDS<sup>(\*)</sup>

by

ANGELO MIELE<sup>(\*\*)</sup> and GARY R. SAARIS<sup>(\*\*\*)</sup>

SUMMARY

This paper refers to a body whose length and base area are given and considers the problem of determining the transversal contour which minimizes the total drag (sum of the pressure drag and the friction drag) under the following assumptions: (a) the body is slender in the longitudinal sense; (b) the longitudinal contour is represented by a power law; (c) the distribution of pressure coefficients obeys Newton's impact law; and (d) the distribution of skin-friction coefficients versus the abscissa is represented by a power law. The indirect methods of the Calculus of Variations are employed and attention is focused first on a class of arcs composed of  $n$  symmetric cycles each covering the angular interval  $2\pi/n$  (or  $2n$  segments each covering the angular interval  $\pi/n$ ) and, then, on the more general case where these symmetry and multiplicity properties are not employed. It is

---

<sup>(\*)</sup>This report supersedes the reports entitled "A Study of the Optimum Transversal Contour of a Body at Hypersonic Speeds Using Indirect Methods, Part I" and "A Study of the Optimum Transversal Contour of a Body at Hypersonic Speeds Using Indirect Methods, Part II".

<sup>(\*\*)</sup>Director of Astrodynamics and Flight Mechanics, Boeing Scientific Research Laboratories.

<sup>(\*\*\*)</sup>Staff Associate, Boeing Scientific Research Laboratories.

shown that the extremal configuration depends strongly on the friction parameter, a parameter which is proportional to the ratio of the cubic root of the average friction coefficient to the average thickness ratio.

Two distinct behaviors are possible depending on whether the friction parameter is supercritical ( $K_f > 1$ ) or subcritical ( $K_f < 1$ ). If the friction parameter is supercritical, the extremal solution is of class I (a circle), and the friction drag accounts for more than two-thirds of the total drag. If the friction parameter is subcritical, the extremal solution is of either class II (any combination of straight-line segments tangent to a basic circle whose radius depends on the length, the base area, the average friction coefficient, and the exponents defining the longitudinal contour and the distribution of skin-friction coefficients) or class III (any combination of circular arcs of radius equal to that of the basic circle and straight-line segments tangent to the circular arcs); furthermore, the friction drag is two-thirds of the total drag. Among the solutions of class II and class III, a particular set is represented by starlike configurations and a further subset by regular polygons.

While the solution is unique in the supercritical case, it is not unique in the subcritical case. More specifically, for each given subcritical friction parameter, an infinite number of equal-drag solutions exist which minimize the drag. For the particular set of starlike configurations, each solution corresponds to a different number of cycles; however, the solution becomes unique if one further constraint is imposed on the problem, such as, the inner radius for bodies of class II and the outer radius for bodies of class III.

Comparison of the drag of extremal solutions with that of bodies of revolution shows that the relative difference is negligible for those subcritical values of the friction parameter which approach one but is appreciable for those values which approach zero. As an example, the extremal configuration exhibits 5% less drag than the body of revolution having equal length and base area for  $K_f = 0.8$ , 25% less drag for  $K_f = 0.6$ , and 57% less drag for  $K_f = 0.4$ .

## 1. INTRODUCTION

In a previous paper (Ref. 1), the transversal contour of a slender body of given length and base area was determined in such a way that the total drag (sum of the pressure drag and the friction drag) is a minimum. Direct methods were employed, and the analysis was confined to a body whose cross section is either a regular polygon or is composed of a basic circle external to which are superimposed symmetric segments of a logarithmic spiral. In this paper, these arbitrary limitations on the transversal contour are removed, and the minimum drag problem is investigated with the indirect methods of the Calculus of Variations. The following basic hypotheses are employed: (a) the body is slender in the longitudinal sense; (b) its longitudinal contour is represented by a power law; (c) the distribution of pressure coefficients is Newtonian; and (d) the distribution of skin friction coefficients versus the abscissa is represented by a power law.

## 2. DETERMINATION OF THE DRAG

Consider two systems of coordinates (Fig. 1): a Cartesian coordinate system  $x, y, z$  and a cylindrical coordinate system  $r, \theta, z$ . With regard to the Cartesian coordinate system, the  $z$ -axis is identical with the undisturbed flow direction, and the  $xy$ -plane is perpendicular to the  $z$ -axis. For the cylindrical coordinate system,  $r$  is the distance of any point from the  $z$ -axis, and  $\theta$  measures the angular position of this point with respect to the  $zx$ -plane. Next, denote by  $\bar{u}_r, \bar{u}_\theta, \bar{u}_z$  the unit vectors of the cylindrical coordinate system, and observe that the direction of  $\bar{u}_z$  is the same as the undisturbed flow direction. Also, denote by  $\bar{n}$  the unit vector normal to the infinitesimal element of wetted area  $dS_w$ , positively oriented outward, and by  $\bar{t}$  the unit vector which is tangent to  $dS_w$  and is in the direction of the local flow after impact. Consequently, the aerodynamic drag per unit dynamic pressure is given by

$$\frac{D}{q} = \iint_{S_w} \left[ -C_p \bar{n} \cdot \bar{u}_z + C_f \bar{t} \cdot \bar{u}_z \right] dS_w \quad (1)$$

where

$$C_p = 2(\bar{n} \cdot \bar{u}_z)^2 \quad (2)$$

is the pressure coefficient associated with Newton's impact law and  $C_f$  is the friction coefficient. After it is assumed that the tangent vector is

contained in the plane of the vectors  $\bar{n}$ ,  $\bar{u}_z$  and it is observed that

$$\bar{t} \cdot \bar{u}_z = |\bar{n} \times \bar{u}_z| \quad (3)$$

$$dS_w = \frac{r}{\bar{n} \cdot \bar{u}_r} d\theta dz$$

the aerodynamic drag can be rewritten in the form

$$\frac{D}{q} = \int_0^{2\pi} \int_0^l \frac{r}{\bar{n} \cdot \bar{u}_r} \left[ -2(\bar{n} \cdot \bar{u}_z)^3 + C_f |\bar{n} \times \bar{u}_z| \right] d\theta dz \quad (4)$$

where  $l$  is the length of the body. If the geometry of the body is described by the equation

$$f(r, \theta, z) = 0 \quad (5)$$

the unit normal vector and the gradient of the function  $f$  satisfy the relationship

$$\bar{n} = \frac{\nabla f}{|\nabla f|} = \frac{f_r \bar{u}_r + (f_\theta/r) \bar{u}_\theta + f_z \bar{u}_z}{[f_r^2 + (f_\theta/r)^2 + f_z^2]^{1/2}} \quad (6)$$

which implies that

$$\bar{n} \cdot \bar{u}_z = \frac{f_z}{[f_r^2 + (f_{\theta}/r)^2 + f_z^2]^{1/2}}$$

$$|\bar{n} \times \bar{u}_z| = \left[ \frac{f_r^2 + (f_{\theta}/r)^2}{f_r^2 + (f_{\theta}/r)^2 + f_z^2} \right]^{1/2} \quad (7)$$

$$\bar{n} \cdot \bar{u}_r = \frac{f_r}{[f_r^2 + (f_{\theta}/r)^2 + f_z^2]^{1/2}}$$

Consequently, Eqs. (4) and (7) lead to the following relationship between the aerodynamic drag per unit dynamic pressure and the geometry of the body:

$$\frac{D}{q} = \int_0^{2\pi} \int_0^l \frac{r}{f_r} \left[ -\frac{2f_z^3}{f_r^2 + (f_{\theta}/r)^2 + f_z^2} + C_f \sqrt{f_r^2 + (f_{\theta}/r)^2} \right] d\theta dz \quad (8)$$

which, because of the slender body approximation  $(f_z/f_r)^2 \ll 1$ , reduces to

$$\frac{D}{q} = \int_0^{2\pi} \int_0^l \frac{r}{f_r} \left[ -\frac{2f_z^3}{f_r^2 + (f_{\theta}/r)^2} + C_f \sqrt{f_r^2 + (f_{\theta}/r)^2} \right] d\theta dz \quad (9)$$

Because of hypothesis (b), the longitudinal contour of the body is represented by the power law

$$f(x, \theta, z) = r - \left(\frac{z}{l}\right)^m R(\theta) = 0 \quad (10)$$

where  $m$  is an arbitrarily prescribed exponent and  $R(\theta)$  is a function which describes the geometry of the base contour (Fig. 1). Furthermore, because of hypothesis (d), the distribution of friction coefficients is represented by (Ref. 2)

$$C_f = C_{fa} (1 - \alpha) \left(\frac{l}{z}\right)^\alpha \quad (11)$$

where  $C_{fa}$  is the average value of the friction coefficient over the entire length of the body and  $\alpha$  is a constant whose typical values are 0 for the idealized model in which the friction coefficient is constant, 1/5 for the turbulent flow model, and 1/2 for the laminar flow model. In the light of these hypotheses, the aerodynamic drag per unit dynamic pressure becomes<sup>(\*)</sup>

---

(\*) From Eq. (12), it appears that the exponents defining the longitudinal contour and the distribution of skin-friction coefficients must satisfy the inequalities  $m > 1/2$  and  $\alpha < 1$ .

$$\frac{D}{q} = \int_0^{2\pi} \left[ \frac{m^3}{l^2(2m-1)} \frac{R^6}{R^2 + \dot{R}^2} + \frac{C_{fa}(1-\alpha)l}{m+1-\alpha} \sqrt{R^2 + \dot{R}^2} \right] d\theta \quad (12)$$

where the dot sign denotes a derivative with respect to the argument  $\theta$ .

The associated base area is given by

$$S = \frac{1}{2} \int_0^{2\pi} R^2 d\theta \quad (13)$$

### 3. FORMULATION OF THE PROBLEM

Prior to the formulation of the minimum drag problem, it is convenient to introduce the dimensionless base radius

$$\rho = \frac{R}{l} = \left[ \frac{2(m+1-\alpha)}{(2m-1)(1-\alpha) C_{fa}} \right]^{1/3} \quad (14)$$

as well as the drag parameter and the friction parameter

$$K_D = \frac{D}{2\pi\eta l^2} \frac{m}{(2m-1)^{1/3}} \left[ \frac{2(m+1-\alpha)}{(1-\alpha) C_{fa}} \right]^{4/3} \quad (15)$$

$$K_f = \frac{l}{m} \left( \frac{\pi}{S} \right)^{1/2} \left[ \frac{(2m-1)(1-\alpha) C_{fa}}{2(m+1-\alpha)} \right]^{1/3}$$

the second of which is proportional to the ratio of the cubic root of the average friction coefficient to the average thickness ratio. After the relationships (12) and (13) are rewritten as<sup>(\*)</sup>

---

<sup>(\*)</sup> The subscript i denotes the initial point and the subscript f, the final point.

$$2\pi K_D = \int_{\theta_1}^{\theta_f} \left[ \frac{\rho^6}{\rho^2 + \dot{\rho}^2} + 2 \sqrt{\rho^2 + \dot{\rho}^2} \right] d\theta \quad (16)$$

$$\frac{2\pi}{K_f^2} = \int_{\theta_1}^{\theta_f} \rho^2 d\theta$$

and after the end conditions are expressed in the form

$$\theta_1 = 0, \quad \theta_f = 2\pi, \quad \rho_1 = \rho_f \quad (17)$$

the problem of minimizing the drag for a given length and base area is formulated as follows: "In the class of functions  $\rho(\theta)$  which are consistent with the isoperimetric constraint (16-2) and the end conditions (17), find that special function such that the integral (16-1) is minimized".

### 3.1. Necessary Conditions

If an undetermined, constant Lagrange multiplier is introduced and the fundamental function is written as (Ref. 3)

$$F(\rho, \dot{\rho}, \lambda) = \frac{\rho^6}{\rho^2 + \dot{\rho}^2} + 2 \sqrt{\rho^2 + \dot{\rho}^2} + \lambda \rho^2 \quad (18)$$

it can be recognized that the previous problem is equivalent to that of minimizing the integral

$$I = \int_{\theta_1}^{\theta_2} F(\rho, \dot{\rho}, \lambda) d\theta \quad (19)$$

subject to the isoperimetric constraint (16-2) and the end conditions (17).

Hence, the Euler-Lagrange equation is given by

$$\frac{d}{d\theta} \left( \frac{\partial F}{\partial \dot{\rho}} \right) - \frac{\partial F}{\partial \rho} = 0 \quad (20)$$

where

$$\frac{\partial F}{\partial \dot{\rho}} = \frac{2\dot{\rho}}{\sqrt{\rho^2 + \dot{\rho}^2}} \left[ 1 - \left( \frac{\rho^4}{\rho^2 + \dot{\rho}^2} \right)^{3/2} \right] \quad (21)$$

Since the fundamental function is formally independent of the argument  $\theta$ , this Euler-Lagrange equation admits the first integral

$$F - \dot{\rho} = C \quad (22)$$

where  $C$  is a constant and where the function  $\dot{\rho}$  is defined as

$$\Phi(\rho, \dot{\rho}) = \dot{\rho} \frac{\partial F}{\partial \dot{\rho}} = \frac{2\dot{\rho}^2}{\sqrt{\rho^2 + \dot{\rho}^2}} \left[ 1 - \left( \frac{\rho^4}{\rho^2 + \dot{\rho}^2} \right)^{3/2} \right] \quad (23)$$

This first integral must be solved for boundary conditions consistent with the transversality condition

$$\left[ \left( F - \dot{\rho} \frac{\partial F}{\partial \dot{\rho}} \right) d\theta + \frac{\partial F}{\partial \rho} d\rho \right]_1^f = 0 \quad (24)$$

which must be satisfied identically for any system of differentials consistent with the end conditions (17). Therefore, it implies that

$$\left( \frac{\partial F}{\partial \dot{\rho}} \right)_1 = \left( \frac{\partial F}{\partial \dot{\rho}} \right)_f \quad (25)$$

Incidentally, the solution may or may not involve angular discontinuities depending on the values of the average friction coefficient, the base area, the length, and the exponents defining the longitudinal contour and the distribution of skin-friction coefficients. Should angular discontinuities be present, the Erdmann-Weierstrass corner conditions<sup>(\*)</sup>

---

<sup>(\*)</sup> The symbol  $\Delta(\dots)$  denotes the difference between quantities evaluated after the corner and before the corner.

$$\Delta \left( F - \dot{\rho} \frac{\partial F}{\partial \dot{\rho}} \right) = \Delta \left( \frac{\partial F}{\partial \dot{\rho}} \right) = 0 \quad (26)$$

must be satisfied at every corner point. In particular, they imply that the integration constant C has the same value for every subarc composing the extremal arc. Finally, the application of the Legendre test indicates that the following necessary condition must be satisfied everywhere along the arc minimizing the drag:

$$\frac{\partial^2 F}{\partial \dot{\rho}^2} = \frac{2\dot{\rho}^2}{(\dot{\rho}^2 + \dot{\rho}^2)^{3/2}} \left[ 1 + \dot{\rho}^4 \frac{3\dot{\rho}^2 - \dot{\rho}^2}{(\dot{\rho}^2 + \dot{\rho}^2)^{3/2}} \right] \geq 0 \quad (27)$$

### 3.2. Symmetry and Multiplicity Properties

Inspection of the functions F and  $\phi$  appearing in the first integral (22) shows that they involve only even powers of  $\dot{\rho}$  and do not involve the argument  $\theta$  explicitly. This means that, if the function  $\rho = \rho(\theta)$  is a particular solution of the Euler-Lagrange equation, then the functions

$$\rho = \rho(-\theta), \quad \rho = \rho(\theta + \text{Const}) \quad (28)$$

are also particular solutions. Eq. (28-1) expresses a symmetry property, since it allows one to obtain from a given extremal shape an infinite number of equal-drag shapes by drawing the mirror image of the original shape with respect to any arbitrary reference direction. Eq. (28-2) expresses a

multiplicity property, since it allows one to obtain from a given extremal shape an infinite number of equal drag shapes by rotating the original shape through an arbitrary angle around the z-axis. Furthermore, combined use of Eqs. (28-1) and (28-2) shows that there exists a class of variational solutions composed of  $n$  identical cycles each of which covers the angular interval  $2\pi/n$  and is symmetric with respect to the radial line joining the origin of the polar coordinate system with the peak point of the cycle. Since these special solutions are particularly amenable to an analytical approach, their properties shall be investigated in Section 4. Then, the more general case is considered in Section 5.

#### 4. MULTIPLE AND SYMMETRIC SOLUTIONS

We shall now restrict the analysis to the class of bodies composed of  $n$  identical cycles; by hypothesis, each cycle involves a pair of symmetric segments, and each segment does not involve corners. The total number of segments is  $2n$ ; each covers the angular interval  $\pi/n$  and yields the same contribution to the drag and the enclosed area. Consequently, the integral to be extremized and the isoperimetric constraint can be rewritten in the form

$$2\pi K_D = \int_{\theta_i}^{\theta_f} 2n \left[ \frac{\rho^6}{\rho^2 + \dot{\rho}^2} + 2 \sqrt{\rho^2 + \dot{\rho}^2} \right] d\theta \quad (29)$$

$$\frac{2\pi}{K_f} = \int_{\theta_i}^{\theta_f} 2n \rho^2 d\theta$$

where

$$\theta_i = 0, \quad \theta_f = \pi/n \quad (30)$$

and where the terminal radii are unconstrained. Clearly, the minimum drag problem consists of minimizing the integral

$$I = \int_{\theta_i}^{\theta_f} 2n F(\rho, \dot{\rho}, \lambda) d\theta \quad (31)$$

subject to the isoperimetric constraint (29-2) and the end conditions (30) with the following understanding: the object of the minimization procedure

is to find not only the equation of each segment but also the number of segments  $2n$  and, hence, the interval of integration  $\Delta\theta = \pi/n$ .

Concerning the optimization of the shape of each segment, the Euler-Lagrange equation (20) is still valid and admits the first integral (22). This first integral must be solved for boundary conditions consistent with the transversality condition (24) which must be satisfied identically for every system of differentials consistent with the end conditions (30). Therefore, it implies that

$$\left(\frac{\partial F}{\partial \dot{\rho}}\right)_i = \left(\frac{\partial F}{\partial \dot{\rho}}\right)_f = 0 \quad (32)$$

and that

$$F_i = F_f = C \quad (33)$$

Furthermore, if the first integral (22) is integrated over the interval  $\Delta\theta$  and Eq. (33) is accounted for, one obtains the expression

$$\int_{\theta_i}^{\theta_f} F d\theta - \int_{\theta_i}^{\theta_f} F d\theta = \frac{\pi}{n} C = \frac{\pi}{n} F_f \quad (34)$$

With regard to the optimization of the number of segments, the theorem of differentiation under the integral sign is applied, that is, the deriva-

tive of the integral (31) with respect to the parameter  $n$  is calculated and the result is set equal to zero. This operation yields the relationship

$$\int_{\theta_i}^{\theta_f} F d\theta - \frac{\pi}{n} F_f = 0 \quad (35)$$

which, if combined with Eq. (34), shows that the following integral condition must be satisfied by the optimum contour:

$$\int_{\theta_i}^{\theta_f} \Phi d\theta = 0 \quad (36)$$

where, owing to the boundary conditions of the problem,

$$\Phi_i = \Phi_f = 0 \quad (37)$$

From the last two equations, it appears that some fundamental information on the nature of the optimum shape can be obtained by investigating the properties of the function  $\Phi$  in the  $\rho\dot{\rho}$ -domain (Fig. 2). Clearly,  $\Phi = 0$  along the arc composed of the subarc<sup>(\*)</sup>

$$\dot{\rho} = 0 \quad (38)$$

---

(\*) The Legendre condition (27) shows that Eq. (38) is valid for  $\rho \leq 1$  only.

ending at  $\rho = 1$  and the subarc<sup>(\*)</sup>

$$\psi(\rho, \dot{\rho}) = \dot{\rho}^2 + \rho^2 - \rho^4 = 0 \quad (39)$$

beginning at  $\rho = 1$ . Furthermore, this function is positive to the left of the line  $\psi = 0$  and negative to the right.

Assuming, then, that the initial point and the final point are arbitrarily located on the line  $\dot{\rho} = 0$ , three classes of bodies must be analyzed (Fig. 2): (I) bodies with both end points on the line  $\dot{\rho} = 0$ , (II) bodies with both end points on the line  $\psi = 0$ , and (III) bodies with the initial point on the line  $\dot{\rho} = 0$  and the final point on the line  $\psi = 0$ . Mathematically speaking, these classes are indicated as follows:

$$\begin{aligned} \text{Class I: } & \dot{\rho}_1 = 0, \quad \dot{\rho}_f = 0 \\ \text{Class II: } & \psi_1 = 0, \quad \psi_f = 0 \\ \text{Class III: } & \dot{\rho}_1 = 0, \quad \psi_f = 0 \end{aligned} \quad (40)$$

For each class, the following subcases need to be examined: (a) the function  $\psi$  does not change sign along the integration contour; (b) the function  $\psi$  does change sign and, therefore, vanishes not only at the end points but also at some intermediate points; and (c) the function  $\psi$  is zero at every point between the end points. The following lemmas are of assistance in finding the solution:

---

<sup>(\*)</sup> The Legendre condition (27) shows that Eq. (39) is valid for  $\rho \geq 1$  only.

Lemma 1. The function  $\Phi$  cannot have a constant, positive or negative, sign along the integration contour. Should  $\Phi$  have a constant sign, the optimum condition (36) would be violated.

Lemma 2. The integration contour may cross the line  $\Phi = 0$  at either at one point or at infinite points but not at any intermediate number of points. Should crossings occur, the first integral (22) and Eq. (39) would be simultaneously valid at all points of intersection with the implication that, at these points,

$$\rho^2 = \frac{C}{\lambda + 3} \quad (41)$$

Now, if the numerator and the denominator of Eq. (41) do not vanish simultaneously, Eq. (41) can be satisfied for only one value of  $\rho$ . On the other hand, if the numerator and the denominator vanish simultaneously, Eq. (41) is satisfied for any value of  $\rho$ .

Applying the previous lemmas, one can find the extremal solution by the following exclusion process: for bodies of class I, contour (a) cannot be extremal because it violates the first lemma; for bodies of class II, contour (a) cannot be extremal since it violates both lemmas, and contour (b) cannot be extremal because it violates the second lemma; for bodies of class III, contour (a) cannot be extremal since it violates the first lemma, and contour (b) cannot be extremal because it violates the second lemma. In conclusion, the extremal arc must necessarily be of type (c) and, therefore, its most general differential equation is

$$\dot{\psi} = 0 \quad (42)$$

The particular differential equations associated with the classes of bodies identified previously are as follows:

$$\begin{aligned} \text{Class I: } \dot{\rho} &= 0 \\ \text{Class II: } \dot{\psi} &= 0 \\ \text{Class III: } \dot{\rho} &= 0 \rightarrow \dot{\psi} = 0 \end{aligned} \quad (43)$$

Regardless of the particular case, the drag parameter, the friction parameter, the integration constant, and the Lagrange multiplier satisfy the relationship

$$K_D = C - \frac{\lambda}{K_f^2} \quad (44)$$

which is obtained by combining Eqs. (18), (29), (34), and (36).

#### 4.1. Bodies of Class I

The contour of these bodies is governed by the differential equation (43-1) which admits the general integral

$$\rho = C_1 \quad (45)$$

where  $C_1$  is a constant. Use of Eqs. (29) supplies the parametric relationships

$$\begin{aligned}
 K_D &= \rho(\rho^3 + 2) \\
 K_f &= \frac{1}{\rho}
 \end{aligned}
 \tag{46}$$

which, after the parameter  $\rho$  is eliminated, lead to the following minimum value for the drag parameter (Fig. 3):

$$K_D = \frac{1 + 2K_f^3}{K_f^4} \tag{47}$$

The associated integration constant and Lagrange multiplier are given by

$$C = \frac{K_f^3 - 1}{K_f^4}, \quad \lambda = -\frac{K_f^3 + 2}{K_f^2} \tag{48}$$

From the Legendre condition, one can see that Eqs. (45) through (48) are valid for  $\rho \leq 1$  only, that is, for  $K_f \geq 1$ . Thus, if one defines  $K_f = 1$  as the critical value of the friction parameter, the following conclusion is reached: the extremal arc is a circle for supercritical values of the friction parameter.

#### 4.2. Bodies of Class II

The contour of these bodies is governed by the differential equation (43-2) whose general integral is

$$\rho = \frac{1}{\cos(\theta + C_2)} \quad (49)$$

where the constant  $C_2$ , to be evaluated from the initial conditions, is given by

$$\rho_1 = \frac{1}{\cos C_2} \quad (50)$$

Elimination of the constant from these equations leads to the result

$$\rho = \frac{\rho_1}{\cos \theta - \sqrt{\rho_1^2 - 1} \sin \theta} \quad (51)$$

which represents the straight-line side of a starlike configuration whose terminal radii satisfy the relationship

$$\rho_f = \frac{\rho_1}{\cos \frac{\pi}{n} - \sqrt{\rho_1^2 - 1} \sin \frac{\pi}{n}} \quad (52)$$

In order to determine the initial radius, the isoperimetric condition (29-2) must be combined with the shape equation (49) to yield

$$\frac{\pi}{nK_f^2} = \int_0^{\pi/n} \frac{d\theta}{\cos^2(\theta + C_2)} = \tan\left(\frac{\pi}{n} + C_2\right) - \tan C_2 \quad (53)$$

This equation, together with Eq. (50), supplies the relationship (Fig. 4)

$$K_f = \frac{1}{\rho_1} \left[ \frac{\pi}{n} \left( \cot \frac{\pi}{n} - \sqrt{\rho_1^2 - 1} \right) \right]^{1/2} \quad (54)$$

from which it is clear that, for a given friction parameter, the boundary value problem does not admit a unique solution but rather an infinite number of solutions, that is, one initial radius for each integer value of the number of cycles. The corresponding final radius is presented in Fig. 5 versus the friction parameter for several values of the number of cycles.

After the initial radius is eliminated from Eqs. (51) and (54), the geometry of the optimum shape can be rewritten in the functional form

$$\rho = \rho(\theta, K_f, n) \quad (55)$$

which is illustrated in Figs. 6 and 7. In Fig. 6, the friction parameter is held at the constant value  $K_f = 0.778$ , and the number of cycles is varied. In Fig. 7, the number of cycles is held at the constant value  $n = 4$ , and the friction parameter is varied.

It should be noted that solutions of class II exist if, and only if, the

relationship (41) is satisfied everywhere. Since this is only possible for

$$C = 0, \quad \lambda = -3 \quad (56)$$

use of Eq. (44) yields the following expression for the minimum drag parameter (Fig. 3):

$$K_D = \frac{3}{K_f} \quad (57)$$

Since this relationship is independent of the number of cycles and the initial radius, one concludes that all of the extremal solutions corresponding to a given value of the friction parameter have the same drag. Furthermore, because of Eqs. (29-1) and (42-2), each solution is such that the friction drag is two-thirds of the total drag. Finally, from the Legendre condition, one can see that Eqs. (49) through (57) are valid for  $\rho \geq 1$  only. If this statement is combined with the isoperimetric condition (29-2) and the mean value theorem is applied, one concludes that starlike solutions of class II are possible for  $K_f \leq 1$  only, that is, for subcritical values of the friction parameter.

Polygonal solutions. The present starlike solutions contain polygonal solutions as a particular case. For  $\rho_1 = 1$ , Eq. (51) reduces to

$$\rho = \frac{1}{\cos \theta} \quad (58)$$

which is the equation of the side of a regular polygon circumscribed on the circle  $\rho = 1$ . The number of sides (i.e., cycles) of the polygon is the lowest among all the starlike solutions of class II corresponding to a given value of the friction parameter and is to be determined from Eq. (54) which reduces to (Fig. 8)

$$K_f = \sqrt{\frac{\pi}{n} \cot \frac{\pi}{n}} \quad (59)$$

Clearly, these polygonal solutions are physically realistic only for a discrete set of values of the friction parameter, that is, those values for which  $n$  is an integer. Incidentally, the number of sides increases monotonically with the friction parameter. In particular, for  $K_f \rightarrow 1$ , the number of sides becomes infinitely large, that is, the extremal solution is a circle. On the other hand, for  $K_f \rightarrow 0$ , the number of sides tends to two, that is, the extremal solution is a flat plate.

#### 4.3. Bodies of Class III

The contour of these bodies is governed by the differential equations (43-3) and involves two subarcs: one is circular and the other is a straight line tangent to the circle. Because of continuity considerations, the transition point from the circle to the straight line is located at  $\rho = 1$ , which means that, at this point, the two subarcs are tangent to one another. Analytically, the extremal arc is represented by

$$\rho = 1, \quad 0 \leq \theta \leq \epsilon \quad (60)$$

$$\rho = \frac{1}{\cos(\theta - \epsilon)}, \quad \epsilon \leq \theta \leq \pi/n$$

where  $\epsilon$  is the angular interval corresponding to the circular portion. In particular, the final radius is given by

$$\rho_f = \frac{1}{\cos\left(\frac{\pi}{n} - \epsilon\right)} \quad (61)$$

In order to determine the unknown angle  $\epsilon$ , the isoperimetric condition (29-2) must be combined with the shape equation (60) to obtain (Fig. 9)

$$\frac{\pi}{nK_f^2} = \int_0^\epsilon d\theta + \int_\epsilon^{\pi/n} \frac{d\theta}{\cos^2(\theta - \epsilon)} = \epsilon + \tan\left(\frac{\pi}{n} - \epsilon\right) \quad (62)$$

Elimination of the parameter  $\epsilon$  from the last two equations yields the relationship

$$K_f = \left[ \frac{\pi/n}{\pi/n + \sqrt{\rho_f^2 - 1} - \arctan \sqrt{\rho_f^2 - 1}} \right]^{1/2} \quad (63)$$

which supplies the final radius in terms of the friction parameter and the

number of cycles (Fig. 5). For a given friction parameter, the boundary value problem does not admit a unique solution but rather a finite number of solutions. The particular solution  $\epsilon = 0$  corresponds to a regular polygon and, as such, is governed by Eqs. (58) and (59). The remaining solutions are characterized by a number of cycles less than that of the regular polygon.

After the parameter  $\epsilon$  is eliminated from Eqs. (60) and (62), the geometry of the optimum shape can be rewritten in the functional form (55) which is illustrated in Figs. 10 and 7. In Fig. 10, the friction parameter is held at the constant value  $K_f = 0.93$ , and the number of cycles is varied. In Fig. 7, the number of cycles is held at the constant value  $n = 4$ , and the friction parameter is varied. Incidentally, the minimum drag parameter is still represented by Eq. (57) and is plotted in Fig. 3. Since this relationship is independent of the number of cycles and the final radius, all of the extremal solutions which correspond to a given value of the friction parameter have the same drag. Furthermore, each solution is such that the friction drag is two-thirds of the total drag. Because of the Legendre condition, these solutions are valid for  $\rho \geq 1$  only. If this statement is combined with the isoperimetric condition (29-2) and the mean value theorem is applied, one concludes that starlike solutions of class III are possible for  $K_f \leq 1$  only, that is, for subcritical values of the friction parameter.

#### 4.4. Discussion of the Results

From the previous analysis, it is evident that the friction parameter has a considerable influence on the nature of the extremal solution. If

one defines  $K_f = 1$  as the critical value of the friction parameter, two distinct behaviors are possible depending on whether the friction parameter is supercritical ( $K_f > 1$ ) or subcritical ( $K_f < 1$ ). If the friction parameter is supercritical, the solution is of class I (circular), and the friction drag contributes more than two-thirds of the total drag. If the friction parameter is subcritical, the solution is of either class II (starlike with straight-line segments) or class III (starlike with circular arcs  $\rho = 1$  alternating with straight-line segments tangent to the circular arcs). The polygonal solutions are a subset of either class II solutions or class III solutions which occur only for discrete values of the friction parameter.

While the solution is unique in the supercritical case, it is not unique in the subcritical case. More specifically, for each given value of the friction parameter, there exists an infinite number of extremal solutions of class II and class III. However, the solution becomes unique if some further constraint is imposed on the problem, that is, the initial radius for bodies of class II and the final radius for bodies of class III.

The solutions of class II as well as those of class III are characterized by the same value of the minimum drag; furthermore, the friction drag is two-thirds of the total drag. Hence, the drag of these solutions is less than that of the equivalent body of revolution (subscript R), that is, the body of revolution having equal length and base area (Fig. 3). Specifically, the drag ratio is given by

$$\frac{D}{D_R} = \frac{3K_f^2}{1 + 2K_f^3} \quad (64)$$

and is plotted in Fig. (11) versus the friction parameter. Clearly, the drag reduction associated with the use of starlike cross sections is negligible for values of  $K_f$  near unity but may be appreciable for values of  $K_f$  near zero. Its magnitude is 5% for  $K_f = 0.8$ , 25% for  $K_f = 0.6$ , and 57% for  $K_f = 0.4$ .

## 5. GENERAL SOLUTIONS

The next step in the analysis is to remove the limitations of the previous section, that is, to find the extremal arc without the restriction that the solution be necessarily composed of  $n$  identical, symmetric cycles. Hence, the problem is to find solutions for the first integral (22) subjected to the end conditions (25) and, in the case where discontinuities occur, to find the corner conditions (26). While a straightforward analytical procedure to find the new optimum has not been found, it has been observed that the differential form (42) of the solution for multiple, symmetric bodies is also valid in the most general case. The proof of this statement lies in the fact that any shape governed by the equation  $\dot{\phi} = 0$  satisfies (a) the end conditions (25), (b) the corner conditions (26), and (c) the first integral (22) providing the fundamental function satisfies the relationship

$$F = C \quad (65)$$

everywhere along the extremal arc. It can be verified that each of the three classes of shapes described by Eqs. (43) is consistent with Eq. (65) providing the integration constant and the Lagrange multiplier be defined by Eqs. (48) in the supercritical case and by Eqs. (56) in the subcritical case.

In conclusion, if the friction parameter is supercritical, the extremal solution is still a circle; furthermore, the minimum drag parameter obeys Eq. (47). On the other hand, if the friction parameter is subcritical, any

combination of circular arcs  $\rho = 1$  and straight lines tangent to the circular arcs is an extremal (see Fig. 12 for some typical examples); furthermore, the minimum drag parameter obeys Eq. (57).

In closing, a word of caution is needed with regard to the assumed distribution of pressure coefficients. Since Newton's law is an empirical law which was found to be experimentally valid for convex bodies at moderate hypersonic Mach numbers, the results of this report are satisfactory only for the circular solutions, the polygonal solutions, and the starlike solutions of class III. For the starlike solutions of class II, the acceptability of the results decreases as the concavity of the extremal increases. Therefore, these solutions are indicative of trends only; in particular, the associated aerodynamic drag should be recalculated with more sophisticated fluid mechanics techniques than those employed here.

REFERENCES

1. MIELE, A., "A Study of the Optimum Transversal Contour of a Body at Hypersonic Speeds Using Direct Methods", Boeing Scientific Research Laboratories, Flight Sciences Laboratory, TR No. 64, 1962.
2. MIELE, A. and COLE, J., "A Study of Optimum Slender Bodies in Hypersonic Flow with a Variable Friction Coefficient", Boeing Scientific Research Laboratories, Flight Sciences Laboratory, TR No. 66, 1963.
3. MIELE, A., Editor, "Extremal Problems in Aerodynamics", Academic Press, New York (in publication).
4. CHERNYI, G. G. and GONOR, A. L., "The Determination of Body Shapes of Minimum Drag Using the Newton and the Busemann Pressure Laws", Paper presented at the Symposium on Extremal Problems in Aerodynamics, Boeing Scientific Research Laboratories, Seattle, Washington, 1962.
5. TOOMRE, A., "Zero-Lift Minimum Drag Hypersonic Bodies", Grumman Aircraft Engineering Corporation, Research Department, Report No. RE-110, 1959.

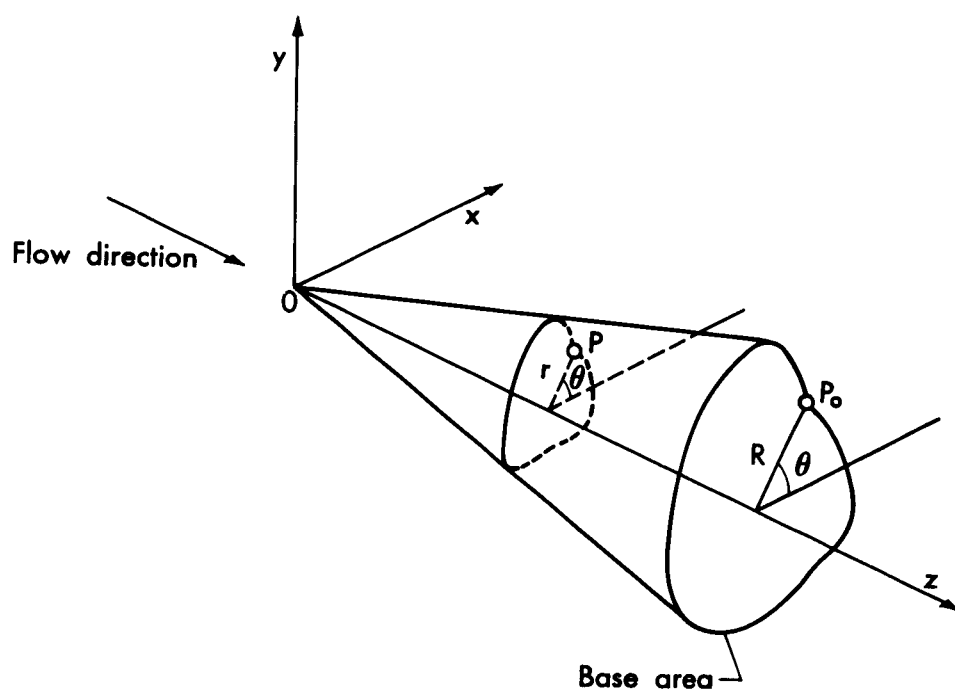


Fig. 1. Coordinate systems

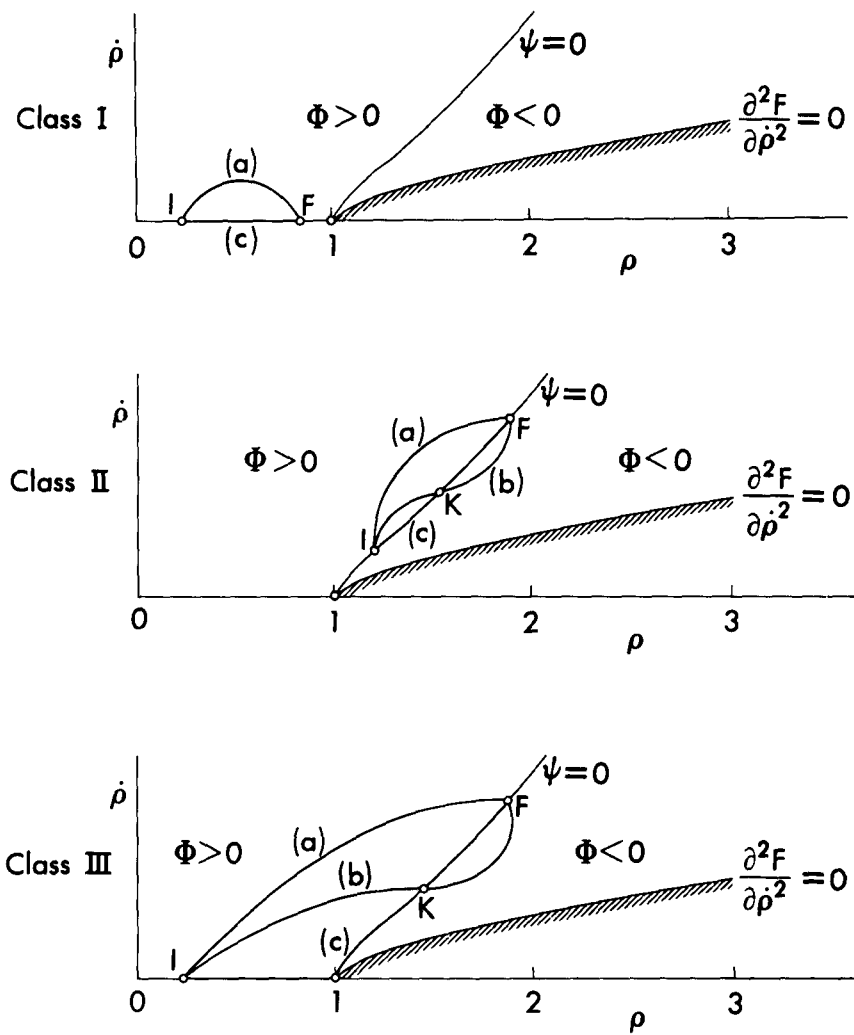


Fig. 2. Alternative integration paths in the  $\rho\dot{\rho}$ -plane.

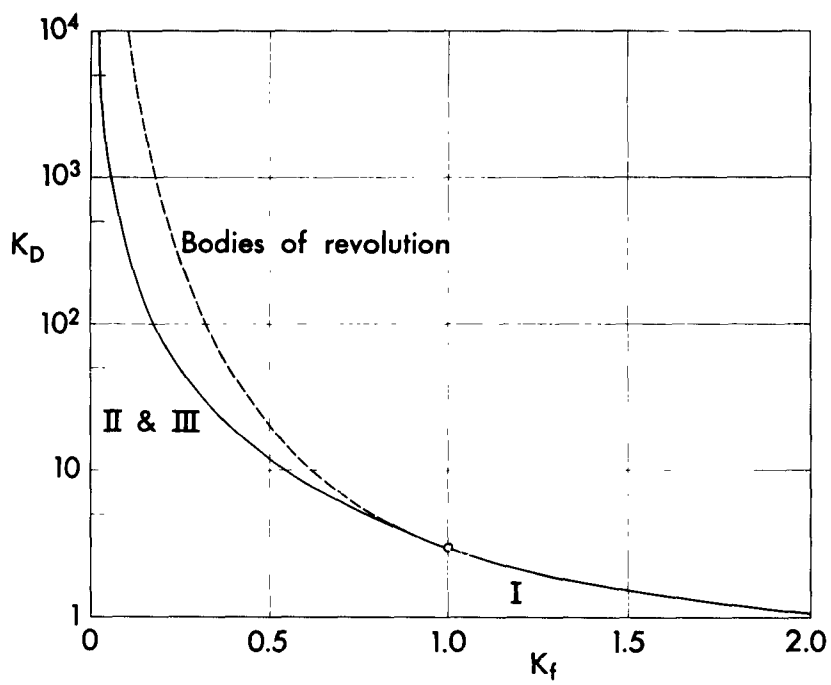


Fig. 3. Minimum drag parameter.

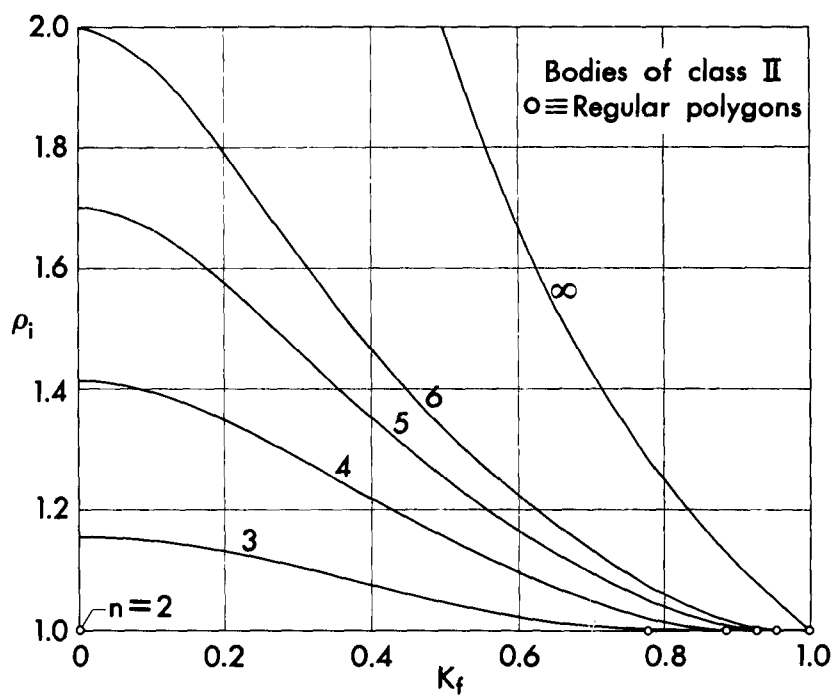


Fig. 4. Initial radius for bodies of class II.

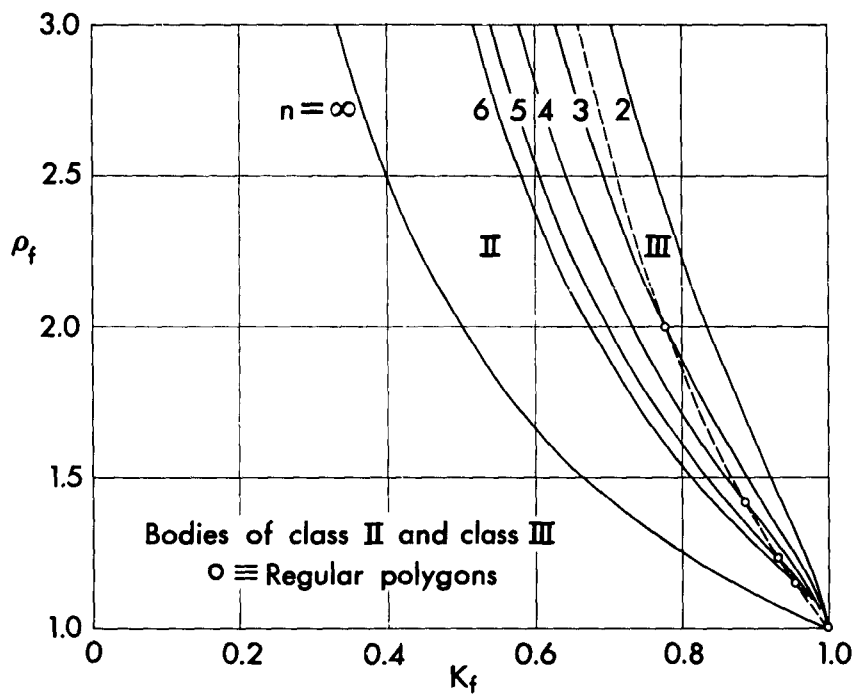


Fig. 5. Final radius for bodies of class II and class III.

Bodies of class II,  $K_f=0.778$

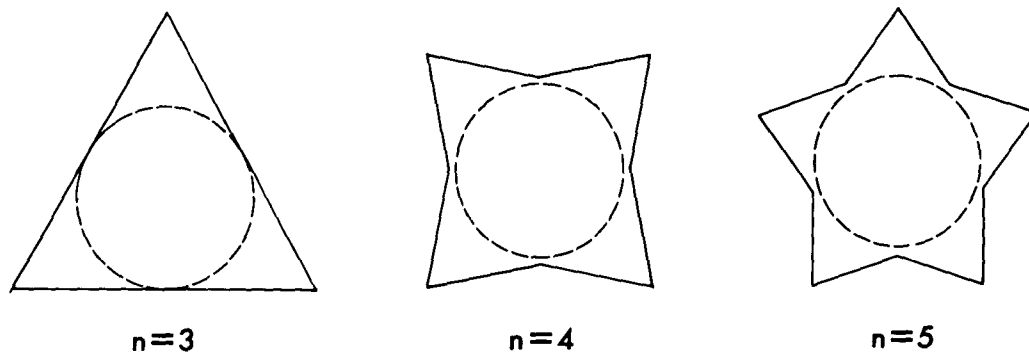


Fig. 6. Examples of solutions of class II.

Bodies of class II and class III,  $n=4$

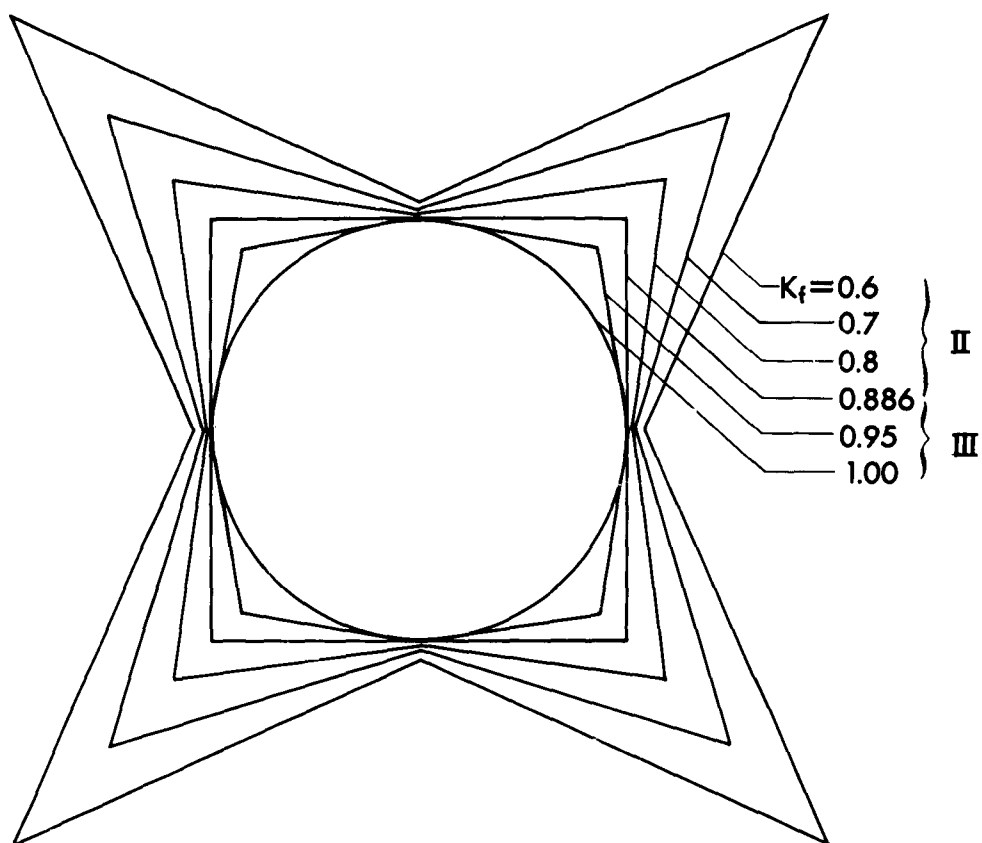


Fig. 7. Examples of solutions of class II and class III.

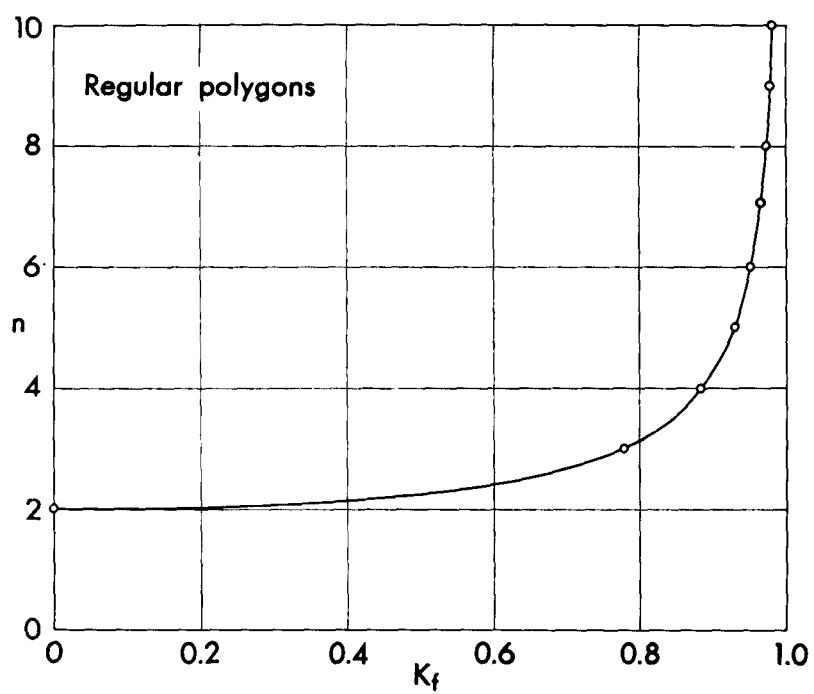


Fig. 8. Optimum number of sides of a body with a polygonal cross section.

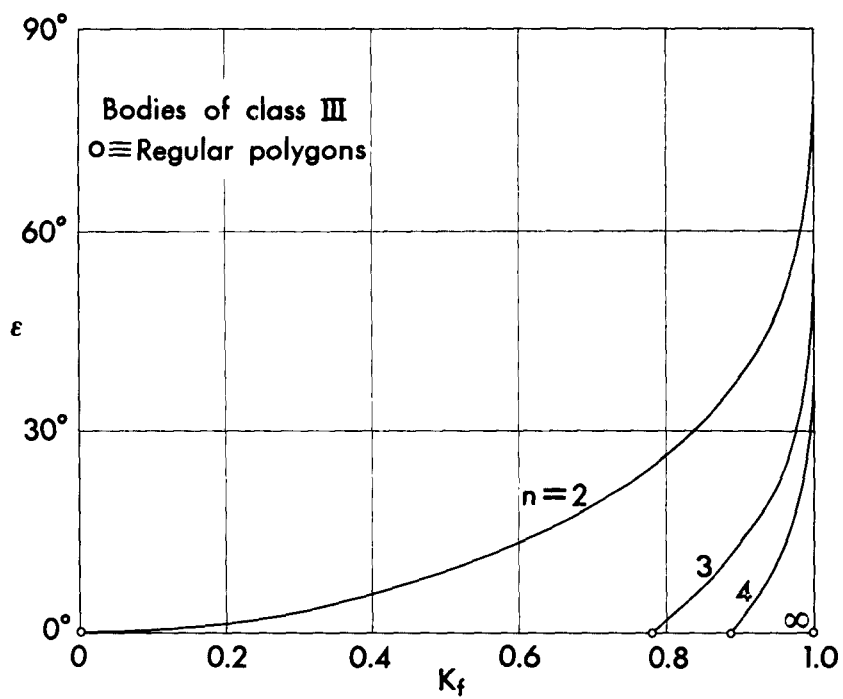


Fig. 9. Angular interval corresponding to the circular portion of bodies of class III.

Bodies of class III,  $K_f=0.93$

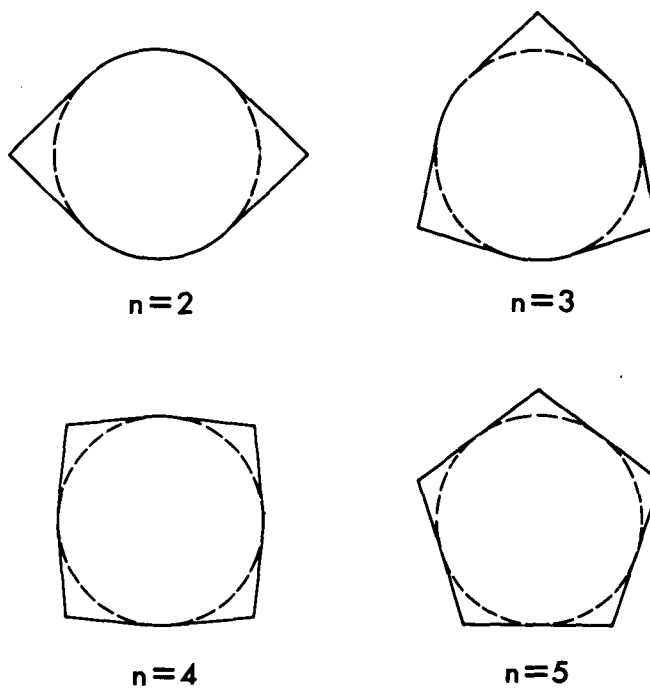


Fig. 10. Examples of solutions of class III.

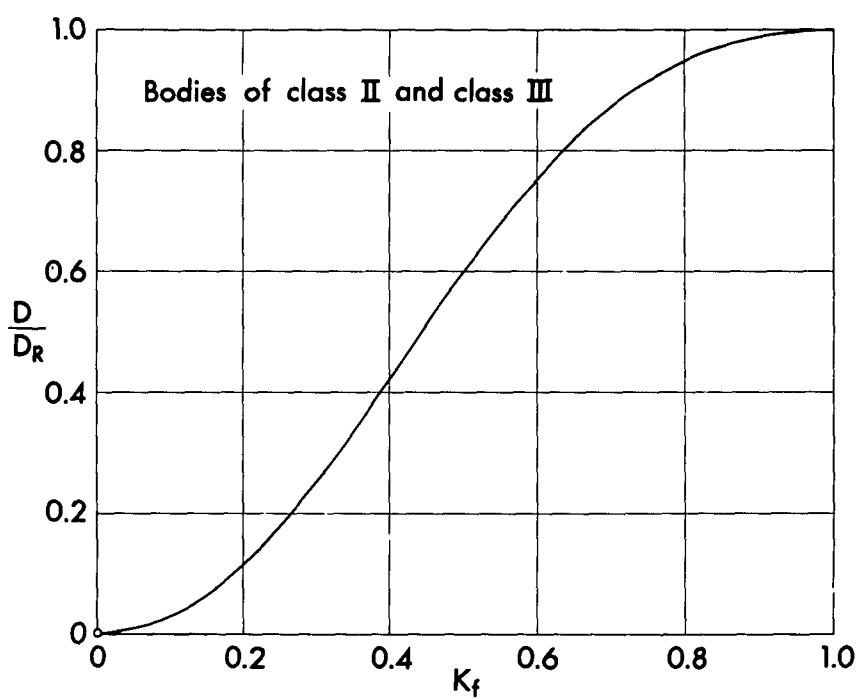


Fig. 11. Ratio of the drag of starlike solutions to that of equivalent bodies of revolution.

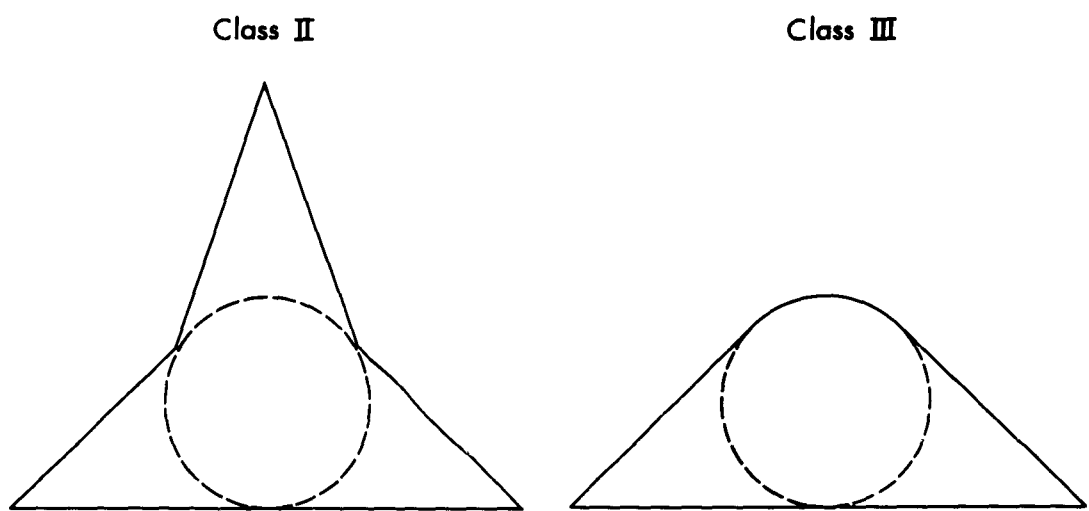


Fig. 12. Examples of solutions of class II and class III.